Acta Materialia 96 (2015) 420–427

Contents lists available at ScienceDirect

Acta Materialia

journal homepage: www.elsevier.com/locate/actamat

Elastocaloric cooling potential of NiTi, Ni_2FeGa, and CoNiAl

Garrett J. Pataky, Elif Ertekin, Huseyin Sehitoglu *

Department of Mechanical Science and Engineering, University of Illinois at Urbana-Champaign, 1206 W. Green St., Urbana, IL 61801, USA

ARTICLE INFO

Article history:
Received 20 February 2015
Revised 2 June 2015
Accepted 4 June 2015
Available online 2 July 2015

Keywords:
Shape memory
Pseudoelasticity
Entropy change
Elastocaloric cooling
Thermography

ABSTRACT

Solid state elastocaloric cooling, the endothermic reversible martensitic phase transformation in shape memory alloys, has the potential to replace vapor compression refrigeration. NiTi, Ni_2FeGa, and CoNiAl shape memory alloys were experimentally investigated to measure the magnitude of temperature change using thermography during uniaxial tensile experiments. Consecutive tensile cycles were also performed, and they revealed a symmetric temperature profile between the two cycles. The unique, dual camera technique of digital image correlation and thermography was utilized to track the transformation bands and temperature gradients to gain insight about the unloading, endothermic process. Fatigue implications, elevated temperature environments, and the theoretical maximum temperature based on entropy change were discussed.

1. Introduction

Solid state refrigeration technology has the potential to reduce the dependence on vapor compression for cooling and refrigeration. Vapor compression relies on refrigerants that are harmful to the environment due to their high global warming potentials (GWP), such as the common hydrofluorocarbon (HFC) HFC-134a which has a GWP of 1430 (100-year) [1]. The GWP indicates how much a chemical will contribute to global warming compared to the same mass of carbon dioxide. Originally, solid state refrigeration was proposed in the 1970s to take advantage of the magnetocaloric effect (MCE) [2]. Since then, much research has been carried out to maximize the potential and applications of the MCE [3]. Elastocaloric cooling in shape memory alloys (SMA) is an alternative solid state refrigeration solution without the necessity of a large magnetic field. The following study focuses on three potential SMAs to meet this demand for a practical, environmentally friendly solution.

Pseudoelastic SMAs have the ability to recover inelastic deformation upon unloading, eliminating the need to heat the material to elicit the shape memory effect [4]. This is of particular interest for elastocaloric cooling as repeated cycling without downtime is desired. In concert with the austenite to martensite transformation, during loading the exothermic stress-induced martensite transformation causes the temperature of the material to increase. When the stress is removed, a temperature decrease (ΔT) occurs due to the endothermic reverse martensitic transformation. The temperature change achieved upon unloading is due to the latent heat absorbed during the reverse martensitic transformation. Pseudoelastic SMAs avoid two issues associated with MCE: the memory effects associated with hysteresis and the narrow temperature range that limits the magnetocaloric effect [5].

The growing interest in elastocaloric cooling is evident when considering the recent increase in literature concerning the topic. Cu–Zn–Al has been featured in several studies to determine the entropy change [6], the experimental temperature change [5], and the heterogeneity of the cooling process [7]. A temperature change of 6 °C was observed [5]. There have also been multiple studies on the well known SMA NiTi. NiTi wires with a diameter of 3 mm were studied and a maximum temperature change of 17 °C was observed [8]. NiTi thin films with a thickness of 20 μm were also investigated and a maximum temperature decrease of 16 °C during unloading was measured via IR camera [9,10]. The present study was performed on NiTi, Ni_2FeGa, and CoNiAl. It is important to note the lack of rare earth elements in all of these studies as this will decrease the cost of the alloys and elevate the usefulness of solid-state refrigeration.

In a crystalline material at finite temperature T, the vibrational modes of the lattice (phonons) contribute to the vibrational entropy $S(T)$. An ideal SMA refrigerant (one that produces the largest ΔT) for elastocaloric cooling would maximize the entropy change: $\Delta S(T) = S_A(T) - S_M(T)$, where $S_A(T)$ is the entropy of the austenite phase and $S_M(T)$ is the entropy of the martensite phase at temperature T. If the tensile experiments are carried out under adiabatic conditions, the total entropy cannot change during the

* Corresponding author.
E-mail address: huseyin@illinois.edu (H. Sehitoglu).

http://dx.doi.org/10.1016/j.actamat.2015.06.011
1359-6454/

phase transition. Thus, the discrepancy $\Delta S(T)$ must be offset by an adiabatic change in temperature ΔT; physically, the temperature drops/increases as the atoms of the lattice absorb/emit phonons during their reorganization [6,11]. As previously specified, this change from martensite to austenite will result in a decrease of temperature in the material. ΔT results from the inverse relationship between ΔS and the specific heat, C_p. Thus, it is imperative to find the SMAs which exhibit the largest ΔS with the smallest C_p. Further information concerning the ΔS of the SMAs in this study will be elaborated on in Section 4.2.

A dual camera combination was utilized in order to simultaneously capture images for digital image correlation while measuring the temperature of the materials. The experimental study spans across two single crystal orientations of NiTi, [148] and [112], two single crystal orientations of Ni_2FeGa, [001] and [011], and the [115] single crystal orientation in CoNiAl. The results presented include the measured temperature change and the theoretical maximum temperature change based on the ΔS for each material and orientation. To these authors' knowledge there have been no studies on the elastocaloric cooling potential of Ni_2FeGa and CoNiAl. This study advances the current state of elastocaloric cooling information by presenting new experimental findings, including repeated cycling showing a consistent ΔT.

2. Experimental details

2.1. Materials

2.1.1. NiTi

The NiTi material was nickel rich with a composition of 50.375 at.%. Single crystals were grown in an inert environment using a Bridgman technique in order to produce the [148] and [112] orientations. The material was solutionized at 920 °C for 24 h in a vacuum furnace and quenched. The specimens were then aged at 550 °C for 1.5 h to produce a microstructure with precipitate of size near 400 nm [12]. This aging also resulted in room temperature (25 °C) pseudoelasticity. Differential scanning calorimetry (DSC) results were obtained by thermally scanning samples at 40 °C/min using a Perkin-Elmer Pyris 1. The characteristic temperatures were found to be $A_f = 0$ °C, $A_s = -15$ °C, $M_s = -55$ °C, and $M_f = -75$ °C. This analysis was repeated on 3 additional samples and consistent results were found. Using ASTM standard E1269, the specific heat was determined to be $C_p = 590$ J/kg K. The parent phase was B2 and upon loading transformed to B19' martensite. A full review of NiTi can be found in [13].

2.1.2. Ni_2FeGa

This alloy was cast at a nominal composition of $Ni_{54}Fe_{19}Ga_{27}$ (at.%). Single crystals were also grown using a Bridgman technique to create the [001] and [011] oriented single crystals. The samples were kept unaged and also exhibited pseudoelastic behavior at room temperature. A DSC analysis on 3 samples provided characteristic temperature values of $A_f = 22$ °C, $A_s = 14$ °C, $M_s = 6$ °C, and $M_f = -3$ °C with a specific heat of $C_p = 460$ J/kg K. The Ni_2FeGa undergoes $L1_2 \rightarrow 10M \rightarrow 14M \rightarrow L1_0$ transformation upon stressing. More information concerning Ni_2FeGa is detailed in [14].

2.1.3. CoNiAl

The third material studied was $Co_{40}Ni_{33.17}Al_{26.83}$ (at.%). Single crystals were grown using the same technique as the previous two materials. The [115] oriented single crystals were aged for 4.5 h at 1275 °C. These specimens produced pseudoelastic results at 100 °C. Other subsequent heat treatments attempted were unable to produce room temperature pseudoelasticity. The DSC results showed consistent characteristic temperatures of $A_f = 45$ °C, $A_s = 22$ °C, $M_s = 16$ °C, and $M_f = 0$ °C and a specific heat of $C_p = 482$ J/kg K. At 100 °C, CoNiAl undergoes transformation from B2 to $L1_0$ martensite with further details presented in [15].

2.2. Temperature change experiments

Tensile experiments were performed on all three materials. The specimens were dog-bone shaped with a width of 3 mm, thickness of 1.75 mm, gage length of 8 mm, and total length of 26 mm. Both sides of the samples were mechanically polished with abrasive paper up to P2400 grit. One side was airbrushed with black paint in order to create a speckle pattern for digital image correlation (DIC). The other side was painted with flat black paint to create uniform emissivity for the IR camera images.

A servo-hydraulic load frame was used for the experiments. Specimens were loaded with the speckle pattern facing a digital camera for DIC images and the solid black side facing the IR camera. The DIC camera was an IMI-202FT digital camera with a resolution of 1600 pixels by 1200 pixels, maximum frame rate of 15 fps, an adjustable lens with a 12× magnification range, and an adapter lens with a 2× magnification. An area of 5 mm by 3 mm was captured with a resolution of 4.25 μm/pixel. A commercially available image correlation program, Vic-2d, was used to perform the DIC analysis. For a description of the DIC technique, see [16]. The IR camera was a closed-cycle cooled DeltaTherm 1550 system from Stress Photonics. The system has the ability to capture images at a rate greater than 1000 fps. The system was calibrated for a temperature range of 15 °C to 115 °C, and images captured were 320 pixels by 256 pixels. An MTS 632.29F-30 5 mm gage length extensometer was also used during the experiments. It could record strains of −10% and 30% for compression and tension respectively with an operating temperature range of −100 °C to 150 °C. The samples were loaded at a strain rate of 10^{-4} s^{-1} and unloaded at a rate of 2×10^{-2} s^{-1}. The faster unloading rate was used in order to approach adiabatic conditions. The full loading and unloading sequence was captured by both cameras (IR and DIC).

3. Results

The endothermic temperature change during the reverse martensitic transformation was measured for NiTi, Ni_2FeGa, and CoNiAl. The tensile stress–strain curves for each of the five orientations are shown in Fig. 1. Unless noted, these experiments were conducted at room temperature. Multiple experiments were

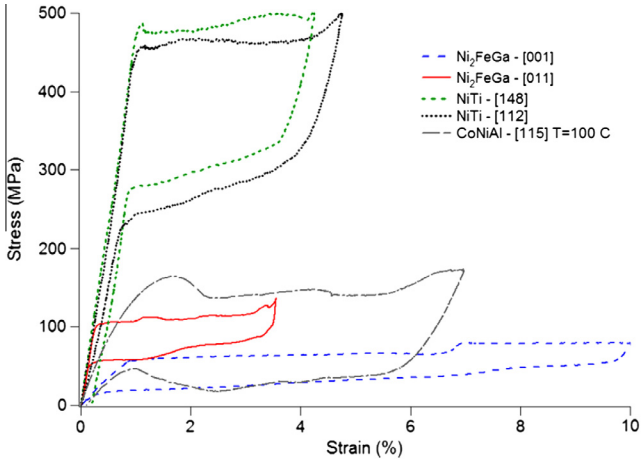

Fig. 1. Tensile stress–strain curves for the experimented shape memory alloys.

performed on each specimen in order to establish the repeatability and consistent ΔT of elastocaloric cooling. The [148] NiTi orientation was strained to 4.25% and a maximum stress of approximately 500 MPa. The [112] NiTi orientation results presented are for 4.75% strain, also a maximum stress of 500 MPa. The Ni_2FeGa experiments exhibited a much lower magnitude of stress. The [011] orientation reached a maximum strain of 3.5% and maximum stress of 135 MPa, while the [001] orientation was strained to 10% with a maximum stress under 100 MPa. The CoNiAl specimen was pulled to 7.0% strain corresponding to a maximum stress of 175 MPa. The pseudoelasticity in each specimen was evident.

3.1. Temperature change

Each temperature change experiment was performed 3–5 times with the same maximum strain and stress. The IR camera captured the entire specimen during the experiment. The average temperature was taken over the entire gage section, and the ΔT reported was measured from the onset of unloading until the specimen was completely unloaded. An animation of the temperature evolution during the experiment for [001] Ni_2FeGa is provided in Video 1 of [17]. The transformations occurred in the gage section during all the experiments, as seen in Video 1 of [17], away from the grips which act as heat sinks.

The findings of this study are presented in Fig. 2. This plot shows the temperature drop for each experiment performed for the 5 orientations. NiTi had the largest ΔT: 14.2 °C for the [148] orientation and 13.3 °C for the [112] orientation. For Ni_2FeGa, the [011] oriented specimen had an average ΔT of 7.6 °C and the [001] specimen had an average of 8.4 °C. The CoNiAl experiment was performed at 100 °C by heating the grips with variable heating cable and allowing the gage section of the specimen to equilibrate at the desired temperature. This specimen had the least ΔT measured, 3.1 °C. Due to the constant flux of heat into the specimen during the experiment, the ΔT measured may not reflect the true temperature change as the conditions were the furthest from adiabatic between the three materials included in this study. These results reflect an expected finding of the ΔT being material dependent, with little dependence on the orientation, because ΔS is a material property.

An additional set of experiments were performed to capture the ΔT of two consecutive tensile cycles. The loading parameters were kept the same as the previous results, with a maximum strain of 3.5% for the [011] oriented Ni_2FeGa specimen and 4.25% for the [148] oriented NiTi specimen. The average gage section temperature versus time plots are given in Fig. 3. Video 2 in [17] shows the temperature change in the two consecutive cycles for the [148] oriented NiTi specimen. Both specimens returned to ambient temperature between loading cycles (26 °C for Ni_2FeGa and 31 °C for NiTi) and show almost identical temperature profiles for both cycles. The small, sharp temperature increases occurring during loading represent the exothermic reactions taking place during the austenite to martensite transformations. The ΔT in both cycles correspond to those found in the previous experiments, approximately 8 °C for Ni_2FeGa and 14 °C for NiTi.

3.2. Temperature change and strain relationship

A large consideration must be given to the fatigue life necessary for solid state refrigeration to be viable. To meet typical refrigeration demands for 10 years, the SMAs must undergo 78 million stress-induced phase transformations [8]. Reducing the strain the material undergoes per cycle could prolong the life of the refrigerant, but the SMA must still undergo an acceptable ΔT in order to act as a refrigerant. A strain versus ΔT experimental matrix was performed on the Ni_2FeGa [001] oriented single crystal. The results are shown in Fig. 4. A minimal ΔT was measured at 2% and less. At a maximum of 3% strain, a temperature drop of approximately 5.5 °C was measured and continued to climb linearly with a ΔT of 6.5 °C at 7% strain. Referencing Fig. 1, 3% strain lies in the middle of the first stress-induced martensite transformation and 7% strain is at the edge of the second stress-induced martensite. A further discussion of the implications of these results will be presented in Section 4.1.

3.3. Transformation bands

The dual camera experimental setup allowed for the simultaneous capture of the strain fields and the sample temperature. This capability provided a means to expound on the relationship between the transformation bands and temperature change during a tensile cycle. The stress–strain curves for the [011] oriented Ni_2FeGa specimen (Fig. 5a) and the [112] oriented NiTi specimen (Fig. 5b) with DIC strain fields and the gage section temperatures are shown in Fig. 5. The isolation of snapshots during the experiments provided a clearer picture of the strain and temperature evolutions.

Starting with the Ni_2FeGa specimen, the sample was at ambient temperature (approximately 29 °C) at 0% strain. As the stress-induced martensitic transformation began, a localized strain

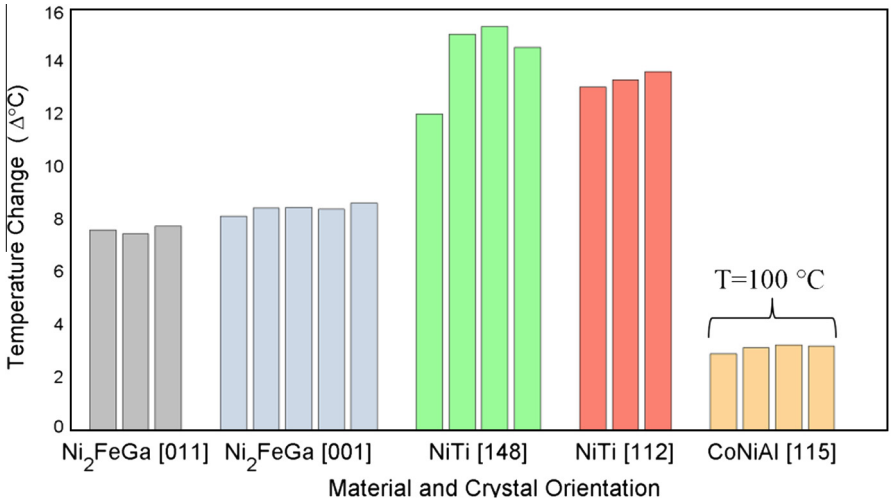

Fig. 2. Temperature change, ΔT, of each experiment for each material.

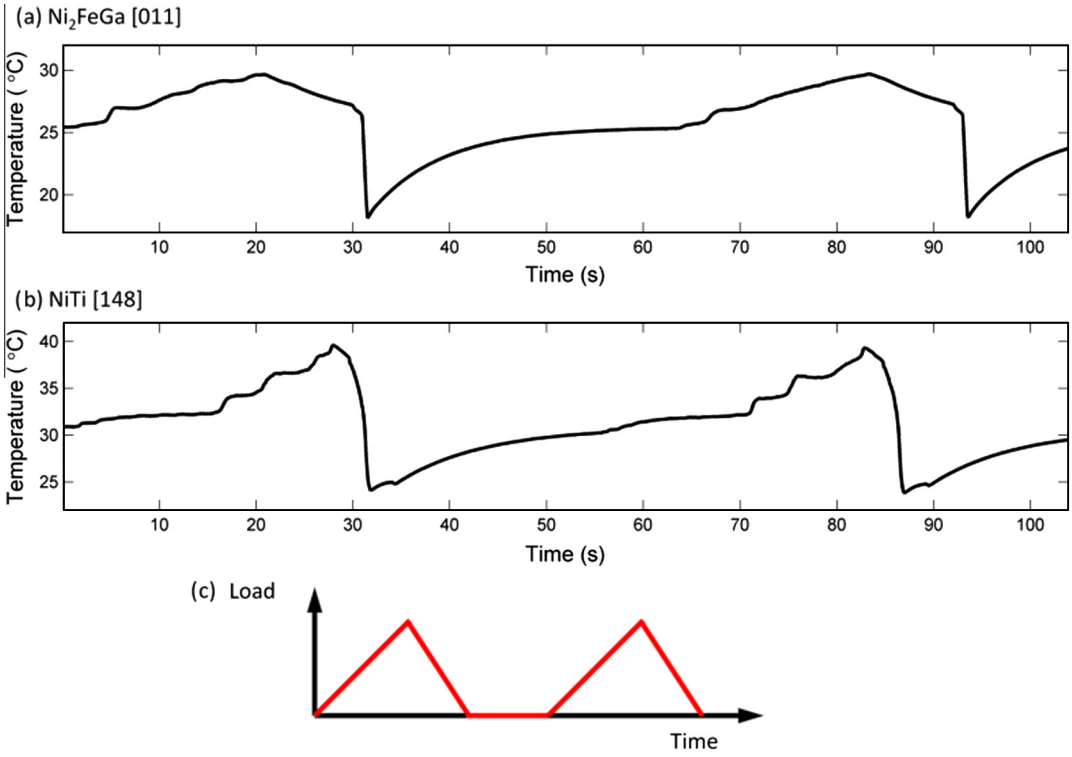

Fig. 3. Temperature versus time plots for the (a) [011] oriented Ni_2FeGa specimen and (b) [148] oriented NiTi specimen. (c) Schematic describing the experiment of two consecutive cycles with a hold period between tensile cycles.

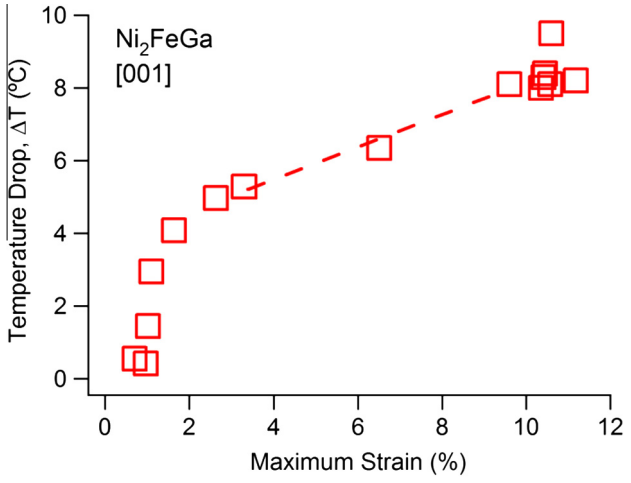

Fig. 4. The temperature change, ΔT, as a function of maximum tensile strain.

band of 4% strain was featured in the center of the gage section with indications of transformation occurring at the top of the gage section as well. The transformation band widened, with a corresponding increase of temperature in the same area, until the maximum strain was achieved and the temperature was 31 °C. Unloading corresponded to a vertical drop of stress and the initiation of the reverse martensitic transformation, as demonstrated by the reduction in strain values. The IR camera images showed an immediate decrease in temperature of approximately 5 °C, with an area of undercooling at the location of the transformation. At the completion of unloading, the sample returned to 0% strain with a ΔT of 8.2 °C. Fig. 5b presents the same trends for the NiTi specimen. In the elastic regime, the specimen temperature was close to ambient temperature and temperature increases were not observed until the stress-induced martensitic transformation occurred. Two transformation bands met and combined as further straining occurred. The exothermal temperature increase was greater in the NiTi sample compared to the Ni_2FeGa sample. During unloading, reverse martensitic transformations occurred at both ends of the specimen and moved toward the middle of the specimen causing the large endothermal ΔT of 13.9 °C.

The exothermic reaction during the loading portion of the tensile cycle differed by material. The Ni_2FeGa specimen saw a maximum increase of 5 °C, but then decreased to 2 °C above ambient temperature before unloading. By contrast, NiTi saw a larger temperature increase of 7 °C during the stress induced martensitic transformation, with no subsequent drop before unloading. This corresponded to a net temperature change, ambient temperature minus minimum temperature, of only 7 °C. The differences between the average and localized temperature change are illustrated in Fig. 5c. The average temperature was 28.4 °C, but along the transformation bands undercooling of approximately 26 °C was observed. These areas are indicated by dotted black lines in Fig. 5c. This discovery indicated that the reversed martensitic transformation has a very local endothermic response, and the surrounding material was dissipating heat into the transformed austenitic material.

4. Discussion

The results of this study contain significant findings for the furthering of elastocaloric cooling. The following section will elucidate the potential of NiTi and Ni_2FeGa for elastocaloric cooling and the ramifications of the differences between the theoretical maximum and experimentally found ΔT values.

4.1. Fatigue considerations for elastocaloric cooling

In order to be a practical alternative to vapor compression, the longevity of the SMAs employed for elastocaloric cooling must be

explored. Since NiTi has been the focus of several studies besides this one [8–10,18–20] and yields the greatest ΔT, it will be the first material of focus. The repeatability and consistency of the ΔT shown in Fig. 3 and Video 2 in [17] are promising findings when considering that MCE has significant changes between the first and second cycles. Other researchers showed that the magnitude of the measured ΔT was reduced by approximately 3.6 °C after only 127 cycles though [18]. Initial discoveries indicated that NiTi could be the most effective SMA for elastocaloric cooling if the ΔT was stabilized, but fatigue life must also be considered. Previous studies on a similar composition, 50.8 at.% Ni, yielded fatigue lives that fall far short of those desired for an elastocaloric cooling refrigerant. The [1 1 2] orientation with a strain range, $\Delta\varepsilon$, of 3% had a fatigue life of 4 cycles or 14 cycles depending on the heat treatment [21]. The same study included the [1 4 8] orientation with minimal improvement with the same strain range, 185 or 224 cycles [21]. Another study on polycrystalline NiTi with the nominal composition of 50.8 at.% Ni presented a table comparing $\Delta\varepsilon$ to the cycles to failure, N_f. The longest fatigue life was 13,495 cycles with a maximum strain of 0.70% and a life of only 340 cycles for a maximum strain of 4.50% [22]. Other studies also corroborate these low fatigue lives at high strains [23,24]. The current study has found that NiTi has the largest ΔT, but the fatigue lives fall far short of the estimated 78 million stress-induced martensitic transformations required for a 10-year life as a refrigerant.

Ni_2FeGa has proven to have a much more promising fatigue life. A previous study of the exact same material showed a fatigue life of 13,579 cycles at a maximum strain of 10% for the [0 0 1] oriented crystal and run out (over 10^7) at 3% strain [25]. It is of great importance to note that these failures were at the filet section, thus the lower bounds of the fatigue life. In the same study, the [0 1 1] oriented specimen had a fatigue life of 6427 cycles at a maximum strain of 1%. This presents a substantial increase in the fatigue life of Ni_2FeGa compared to NiTi. This study presents the first experimental findings concerning the ΔT of Ni_2FeGa and measurements indicated a significant magnitude. The results from Fig. 4 showed that a temperature change of approximately 6 °C is achievable at 4% maximum strain. This was an increase of 1% of $\Delta\varepsilon$ compared to the results in Efstathiou et al. that achieved run out [25]. Another advantage of Ni_2FeGa was the low stresses required to initiate transformation. The [0 0 1] orientation underwent full transformation to a maximum strain of 10% while the stresses remained under 100 MPa. The NiTi specimens both required a stress of 500 MPa to complete transformation. A further analysis of the fatigue implications needs to be investigated including changes in ΔT after repeated cycling, but preliminary results indicate that the much longer fatigue life of Ni_2FeGa points to it as a material which should receive serious consideration for future elastocaloric studies. Furthermore, this SMA does not rely on expensive and scarce rare earth metals.

4.2. Theoretical temperature change considerations

The experimental results observed approach adiabatic conditions, but do not represent the theoretical maximum obtainable temperature change (ΔT_{th}). Two methods of measurement to find ΔT_{th} were employed. Both use the Clausius–Clapeyron relationship given in Eq. (1) to find ΔS, the entropy of transformation per unit volume [4].

$$-\Delta S = \frac{d\sigma}{dT}\varepsilon_0 = -\frac{\Delta H}{T_0} \tag{1}$$

In this expression, $\frac{d\sigma}{dT}$ is the Clausius–Clapeyron slope, ε_0 is the transformation strain, ΔH is the enthalpy of the transformation per unit volume, and T_0 is the thermodynamic equilibrium temperature between the two phases. The quantity $\frac{d\sigma}{dT}$ describes the dependence of the critical stress required to induce martensitic transformation under tension (0.1% strain) on the orientation and temperature. $\frac{d\sigma(M_s)}{dT}$ and $\frac{d\sigma(A_f)}{dT}$ are nearly parallel, therefore, $\frac{d\sigma(M_s)}{dT}$ is an acceptable approximation for $\frac{d\sigma(T_0)}{dT}$ or $\frac{d\sigma}{dT}$ as it is referred to in Eq. (1). Experiments were performed for each of the five orientations included in this study and the results are given in Fig. 6. Lattice deformation theory (LDT) was utilized to find the transformation strain for each material and orientation [26]. To find ΔT_{th}, fully adiabatic conditions were assumed and the theoretical maximum elastocaloric adiabatic temperature change was estimated using Eq. (2) [6].

$$\Delta T_{th} = -\frac{T}{C_p}\Delta S \tag{2}$$

ΔS was found using Eq. (1), T is the ambient temperature (the ambient temperature of each experiment was used as it varied from 25 °C to 36 °C depending on the day of the experiment), and C_p is the specific heat given in Section 2.1 for each material. The calculated ΔT_{th} using the Clausius–Clapeyron slope are given in Table 1.

For the second method to find ΔS, a DSC analysis was performed on four samples of each orientation ranging from 20 mg to 60 mg by scanning at 40 °C/min, and ΔH was found by averaging the areas taken under the DSC curves. Tong and Wayman presented the accepted approximation for T_0 given in Eq. (3) [27].

$$T_0 = \frac{1}{2}(M_s + A_f) \tag{3}$$

The values of M_s and A_f were previously given for each of the materials investigated in Section 2.1. ΔT_{th} was calculated using Eq. (2) and the results using the enthalpy of the transformation are given in Table 2.

As indicated in Tables 1 and 2, the theoretical maximum temperature change was higher than the experimentally found temperature change. The ΔS in Tables 1 and 2 for Ni_2FeGa were consistent with the value reported in the literature [28]. ΔT_{th} being greater than the experimentally found ΔT was consistent with other elastocaloric cooling studies. A difference of 50% was reported for CuZnAl [5] and a difference of 25% was reported for NiTi wires [8]. One explanation focuses on the unloading strain rate as it has a direct impact on ΔT. The quicker the unloading rate, the closer the experiment is to adiabatic conditions. In the study by Mañosa et al., the unloading strain rate was $1.5 \times 10^{-1}\ s^{-1}$ compared to the $2 \times 10^{-2}\ s^{-1}$ in the current study [5]. Precipitates formed during the heat treatment process play a large role in the differences between the two methods used to calculate ΔT_{th}. This was observed as the two methods reported a similar magnitude of ΔT_{th} for Ni_2FeGa, which was experimented on as received, compared to the large differences found for the two heat treated alloys, NiTi and CoNiAl.

4.3. Ambient temperature impact

The inclusion of CoNiAl in this study provided an opportunity to discover the ability of SMAs to be refrigerants in a high temperature environment. CoNiAl was experimented on at a start temperature of 100 °C with an average ΔT of 3.1 °C. Mañosa et al. provided a plot of the elastocaloric and magnetocaloric adiabatic temperature changes as a function of temperature [5]. At 100 °C, only gadolinium, a rare earth element, was reported as having a measured temperature change. The ΔT was stated at approximately 1 °C. This showed that CoNiAl provides a much more viable cooling option in high temperature situations compared to other reported materials.

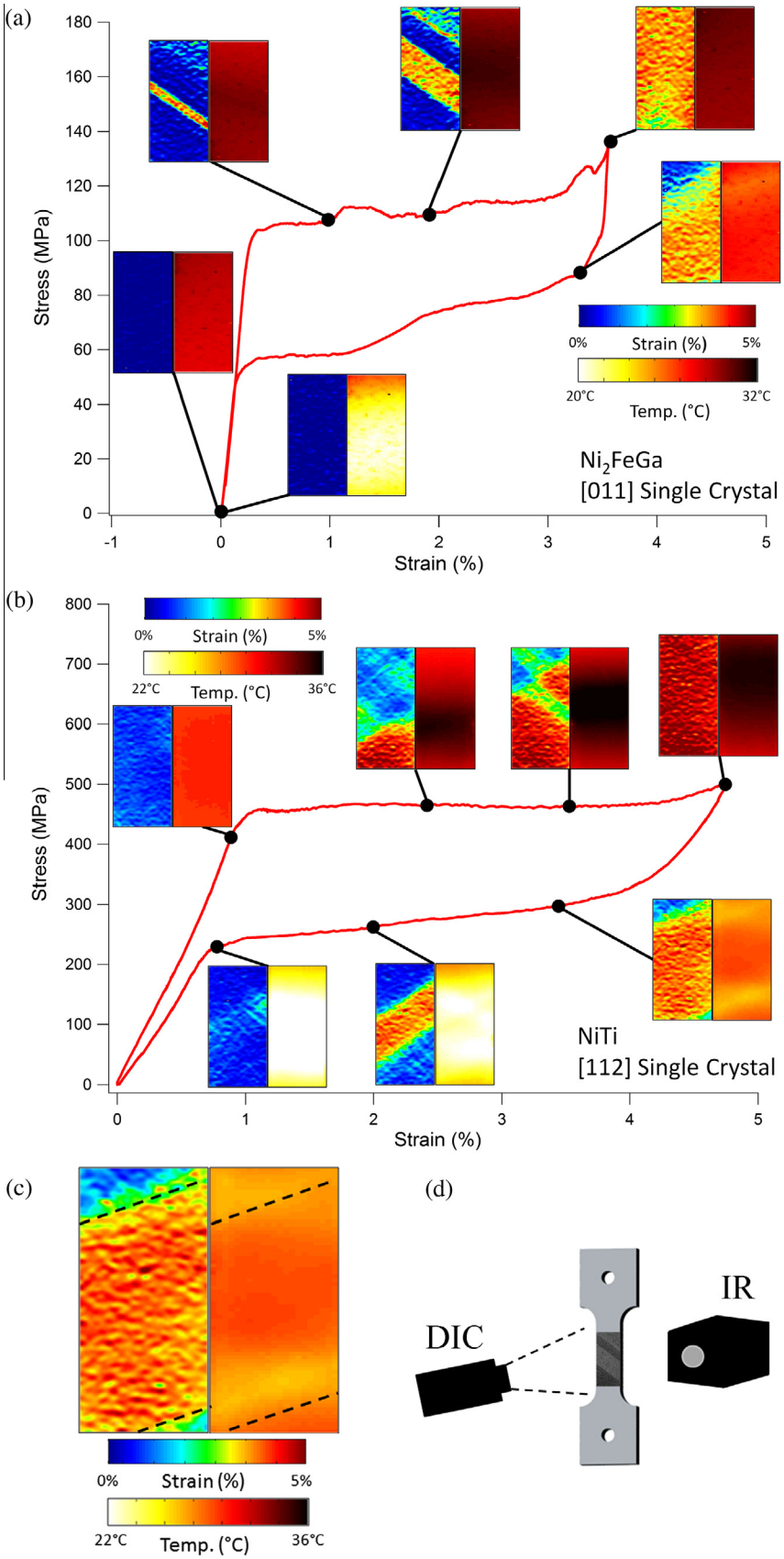

Fig. 5. Tensile stress–strain curves of the (a) [0 1 1] oriented Ni_2FeGa specimen and (b) [1 1 2] oriented NiTi specimen with selected DIC strain fields and temperature gradient of the gage section. (c) During the reverse martensitic transformation in the [1 4 8] NiTi single crystal, the transformation band edges corresponded to a localized undercooling as indicated by the dotted black lines. (d) Schematic of the two camera setup with the DIC camera in front and the IR camera behind the sample.

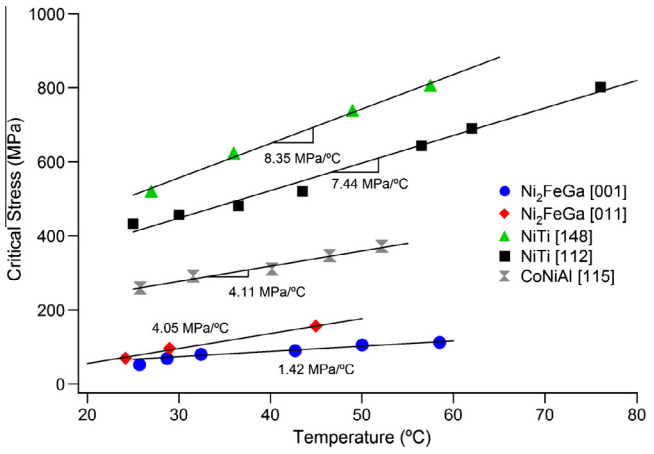

Fig. 6. Critical stress (0.1% strain) as a function of temperature used to find the Clausius–Clapeyron slopes.

Table 1
ΔT_{th} calculated using the Clausius–Clapeyron slope.

	ε_0 (%)	$d\sigma/dT$ {MPa/°C}	ΔS {J/kg K}	C {J/kg K}	T {K}	ΔT_{th} {K}	ΔT {K}
NiTi							
[148]	8.34	8.35	−69.64	590	303	35.76	14.2
[112]	9.5	7.44	−70.68	590	302	36.18	13.3
Ni_2FeGa							
[011]	4.1056	4.05	−16.63	460	302	10.92	7.6
[001]	14.5486	1.42	−20.66	460	309	13.88	8.4
CoNiAl							
[115]	10.71	4.11	−44.02	482	303	27.67	3.1

Table 2
ΔT_{th} calculated using the enthalpy change during transformation.

	T_0 {K}	ΔH {J/g}	ΔS {J/kg K}	C {J/kg K}	T {K}	ΔT_{th} {K}	ΔT {K}
NiTi							
[148]	245.5	12.51	−50.96	590	303	26.17	14.2
[112]	260	10.83	−41.65	590	302	21.32	13.3
Ni_2FeGa							
[011]	288.5	5.14	−17.82	460	302	11.70	7.6
[001]	281	4.51	−16.05	460	309	10.78	8.4
CoNiAl							
[115]	303.5	2.684	−8.84	482	303	5.56	3.1

In addition to the ability to have a significant ΔT, it is desired that a material has a minimal exothermal reaction during the stress induced martensitic transformation, or at the very least one that is dissipated rapidly. In this study, NiTi had the highest measured temperature rise. As a refrigerant, an increase of temperature is a disadvantageous trait for a material. Ni_2FeGa had a minimal increase compared to NiTi with a chronicled longer fatigue life. Further studies on the impact of environmental temperatures need to be performed for both of these alloys in order to compare their ΔT to that of CoNiAl.

5. Conclusions

- An experimental study was carried out on three SMAs in order to measure the adiabatic temperature change. The ΔT was measured experimentally for the first time in Ni_2FeGa (average 8 °C) and CoNiAl (average 3 °C). NiTi measured the highest average ΔT of 14 °C.
- This study identifies a new potential elastocaloric refrigerant, Ni_2FeGa, and underscores its potential advantages for long term operations.
- The ΔT of two consecutive tensile cycles was recorded and the temperature profiles showed a symmetric, consistent temperature change.
- Simultaneous DIC and IR camera measurements during the tensile cycling of SMAs indicated that the reverse martensitic transformations exhibited a localized temperature undercooling.

Acknowledgments

The work is supported by the National Science Foundation, NSF CMMI 14-37106 DMREF grant.

References

[1] G.J.M. Velders, D.W. Fahey, J.S. Daniel, M. McFarland, S.O. Andersen, The large contribution of projected HFC emissions to future climate forcing, Proc. Natl. Acad. Sci. 106 (2009) 10949–10954.
[2] G.V. Brown, Magnetic heat pumping near room temperature, J. Appl. Phys. 47 (1976) 3673–3680.
[3] A.M. Tishin, Y.I. Spichkin, The Magnetocaloric Effect and its Applications, Taylor & Francis, 2003.
[4] K. Otsuka, C.M. Wayman, Shape Memory Materials, Cambridge University Press, 1998.
[5] L. Mañosa, S. Jarque-Farnos, E. Vives, A. Planes, Large temperature span and giant refrigerant capacity in elastocaloric Cu–Zn–Al shape memory alloys, Appl. Phys. Lett. 103 (2013).
[6] E. Bonnot, R. Romero, L. Mañosa, E. Vives, A. Planes, Elastocaloric effect associated with the martensitic transition in shape-memory alloys, Phys. Rev. Lett. 100 (2008) 125901.
[7] E. Vives, S. Burrows, R.S. Edwards, S. Dixon, L. Mañosa, A. Planes, R. Romero, Temperature contour maps at the strain-induced martensitic transition of a Cu–Zn–Al shape-memory single crystal, Appl. Phys. Lett. 98 (2011).
[8] J. Cui, Y. Wu, J. Muehlbauer, Y. Hwang, R. Radermacher, S. Fackler, M. Wuttig, I. Takeuchi, Demonstration of high efficiency elastocaloric cooling with large ΔT using NiTi wires, Appl. Phys. Lett. 101 (2012).
[9] H. Ossmer, C. Chluba, B. Krevet, E. Quandt, M. Rohde, M. Kohl, Elastocaloric cooling using shape memory alloy films, J. Phys: Conf. Ser. 476 (2013).
[10] H. Ossmer, F. Lambrecht, M. Gültig, C. Chluba, E. Quandt, M. Kohl, Evolution of temperature profiles in TiNi films for elastocaloric cooling, Acta Mater. 81 (2014) 9.
[11] X. Moya, S. Kar-Narayan, N.D. Mathur, Caloric materials near ferroic phase transitions, Nat. Mater. 13 (2014) 439–450.
[12] H. Sehitoglu, R. Hamilton, D. Canadinc, X.Y. Zhang, K. Gall, I. Karaman, Y. Chumlyakov, H.J. Maier, Detwinning in NiTi alloys, Metall. Mater. Trans. A 34 (2003) 5–13.
[13] K. Otsuka, X. Ren, Physical metallurgy of Ti–Ni-based shape memory alloys, Prog. Mater Sci. 50 (2005) 511.
[14] R.F. Hamilton, C. Efstathiou, H. Sehitoglu, Y. Chumlyakov, Thermal and stress-induced martensitic transformations in NiFeGa single crystals under tension and compression, Scripta Mater. 54 (2006) 465.
[15] R.F. Hamilton, H. Sehitoglu, C. Efstathiou, H.J. Maier, Y. Chumlyakov, X.Y. Zhang, Transformation of Co–Ni–Al single crystals in tension, Scripta Mater. 53 (2005) 131.
[16] M. Sutton, J.-J. Orteu, H. Schreier, Image Correlation for Shape Motion and Deformation Measurements: Basic Concepts, Theory and Applications, Spring Media, 2009.
[17] G.J. Pataky, E. Ertekin, H. Sehitoglu, Infrared thermography of the elastocaloric effect, Acta Mater., Data in Brief, submitted for publication.
[18] C. Bechtold, C. Chluba, R. Lima de Miranda, E. Quandt, High cyclic stability of the elastocaloric effect in sputtered TiNiCu shape memory films, Appl. Phys. Lett. 101 (2012).
[19] J. Cui, Shape memory alloys and their applications in power generation and refrigeration, MRS Online Proceedings, vol. 1581, Cambridge Journals Online, 2013.
[20] K. Mukherjee, S. Sircar, N.B. Dahotre, Thermal effects associated with stress-induced martensitic transformation in a Ti–Ni alloy, Mater. Sci. Eng. 74 (1985) 75.
[21] K. Gall, N. Yang, H. Sehitoglu, Y. Chumlyakov, Fracture of precipitated NiTi shape memory alloys, Int. J. Fract. 109 (2001) 189–207.
[22] C. Maletta, E. Sgambitterra, F. Furgiuele, R. Casati, A. Tuissi, Fatigue of pseudoelastic NiTi within the stress-induced transformation regime: a modified Coffin–Manson approach, Smart Mater. Struct. 21 (2012).
[23] G. Eggeler, E. Hornbogen, A. Yawny, A. Heckmann, M. Wagner, Structural and functional fatigue of NiTi shape memory alloys, Mater. Sci. Eng., A 378 (2004) 24.

[24] K.N. Melton, O. Mercier, Fatigue of NITI thermoelastic martensites, Acta Metall. 27 (1979) 137.
[25] C. Efstathiou, H. Sehitoglu, P. Kurath, S. Foletti, P. Davoli, Fatigue response of NiFeGa single crystals, Scripta Mater. 57 (2007) 409.
[26] T. Saburi, S. Nenno, The shape memory effect and related phenomena, Solid Solid Phase Transf. (1981) 1455–1479.
[27] H.C. Tong, C.M. Wayman, Characteristic temperatures and other properties of thermoelastic martensites, Acta Metall. 22 (1974) 887.
[28] Y.I. Chumlyakov, I.V. Kireeva, E.Y. Panchenko, E.E. Timofeeva, Z.V. Pobedennaya, S.V. Chusov, I. Karaman, H. Maier, E. Cesari, V.A. Kirillov, High-temperature superelasticity in CoNiGa, CoNiAl, NiFeGa, and TiNi monocrystals, Russ. Phys. J. 51 (2008) 1016–1036.